minerals

MDPI

Article

Removal of Cyanide in Gold Cyanide Residues through Persulfate-Advanced Oxidation Process

Wenwen Han [1,2], Hongying Yang [1,2,*] and Linlin Tong [1,2]

[1] Key Laboratory for Ecological Metallurgy of Multimetallic Mineral (Ministry of Education), Northeastern University, Shenyang 110819, China; hanwenwen_neu@163.com (W.H.); tongll@smm.neu.edu.cn (L.T.)
[2] School of Metallurgy, Northeastern University, Shenyang 110819, China
* Correspondence: yanghy@smm.neu.edu.cn

Abstract: The toxic cyanides in gold cyanide residues produced in the cyanidation process of gold extraction threaten environmental safety and inhibit the recovery of valuable metals. In this study, the removal of cyanide through the persulfate-advanced oxidation process was investigated, and heat activation and ultrasonic activation were tested for cyanide removal. The results showed that cyanide in cyanide residue could be removed by 2.0 wt.% potassium persulfate at pH 10.0 after 60 min reaction with a removal efficiency of 53.47%. The removal efficiency increased to 62.18% at T = 60 °C for heat activation and 74.76% with an ultrasonic power of 100% for ultrasonic activation. The cyanide content in the toxic leaching solution of the residue after the ultrasonic-activated persulfate-advanced oxidation process (3.84 mg/L) reached the national standard of China. Two kinds of free radical scavengers, tert-butanol and methanol, were used to investigate the generation of free radicals. The results showed that both $SO_4^{\bullet -}$ and $HO^{\bullet}$ were produced and accelerated the oxidation of cyanide, and $HO^{\bullet}$ played a major role under alkaline conditions. According to XPS analysis, the oxidation of ultrasonic-activated persulfate focused on cyanide removal rather than pyrite in cyanide residue. More cyanides were transferred from the cyanide residue to the liquid phase, leading to the high efficiency of ultrasonic activation. The ultrasonic-activated persulfate-advanced oxidation process has potential application prospects for the treatment of gold cyanide residues.

Keywords: cyanide removal; gold cyanide residue; persulfate-advanced oxidation; heat activation; ultrasonic activation

check for updates

Citation: Han, W.; Yang, H.; Tong, L. Removal of Cyanide in Gold Cyanide Residues through Persulfate-Advanced Oxidation Process. *Minerals* **2023**, *13*, 613. https://doi.org/10.3390/min13050613

Academic Editor: Rajesh Kumar Jyothi

Received: 29 March 2023
Revised: 18 April 2023
Accepted: 24 April 2023
Published: 28 April 2023

Copyright: © 2023 by the authors. Licensee MDPI, Basel, Switzerland. This article is an open access article distributed under the terms and conditions of the Creative Commons Attribution (CC BY) license (https://creativecommons.org/licenses/by/4.0/).

1. Introduction

Owing to the wide applications of the cyanidation process for gold extraction, the gold industry produces large amounts of waste residue containing high concentrations of cyanide, which is highly toxic and poses a serious threat to the environment and life [1,2]. It has been reported that cyanides could also cause a low flotation recovery of valuable metals in gold cyanide residues and influence the comprehensive utilization of resources [3]. In recent years, cyanide contents in both wastewater and solid waste have been controlled strictly when discharging in most countries around the world [4]. For example, gold cyanide residues cannot be stored or discharged until the total cyanide content in the toxic leaching solution is under 5 mg/L according to technical specification (HJ943-2018, China) [5]. Therefore, the removal of cyanide in gold cyanide residues must be carried out before disposal.

Cyanide can be removed through physical, chemical and biological treatments [6–8], the most widely used of which are chemical methods including acidification [9], alkaline chloride oxidation [10], SO_2—air oxidation [4], hydrogen peroxide oxidation [11] and ozone oxidation [12]. However, the above traditional treatments do not work satisfactorily for cyanide residues due to the high content of stable metal complex cyanides adsorbed on the

surface of some metallic minerals in cyanide residues [13]. Therefore, advanced oxidation processes (AOPs) with a stronger oxidation capacity are tested to treat cyanide residues.

AOPs are an effective method for pollutant degradation that relies on the production of strong oxidizing radicals (such as hydroxyl radicals $HO^{\bullet}$ and sulfate radicals $SO_4^{\bullet -}$) [14,15]. Hydrogen peroxide, ozone and persulfate are commonly used, with redox potentials of 1.77 V, 2.07 V and 2.01 V, respectively. Stronger oxidizing free radicals including $HO^{\bullet}$ and $SO_4^{\bullet -}$ (the redox potential = 1.8~2.7 V, 2.5~3.1 V, respectively) are produced under activation by other energy, such as heat (thermolysis), UV irradiation (photolysis), ionizing irradiation (radiolysis) and chemical electron transfer (catalysis) [16]. Persulfate is gaining importance in AOPs due to its low sensitivity to pH and easy storage as a solid agent. It has been widely used with different activation methods, including carbonaceous material-activated persulfate [17], microwave-activated persulfate [18] and ultrasound-activated persulfate [19]. At present, most of the studies on persulfate-advanced oxidation have focused on organic contaminants, such as bisphenol A [20], valsartan [21], diclofenac [22] and others [23,24], but there has been little definite illustration of the chemistry and kinetics of inorganic substances. Sun et al. [25] studied the treatment of ferricyanide wastewater with persulfate. Moussavi et al. [26] carried out UVC/$S_2O_8^{2-}$ advanced oxidation processes for the degradation of cyanide in wastewater. However, there has been no systematic study on the removal of cyanide in gold cyanide residues through the persulfate-advanced oxidation process.

The main purpose of this study was to investigate cyanide removal from gold cyanide residues through the persulfate-advanced oxidation process. The aim was to study the effects of initial pH, persulfate concentration, reaction time, heat activation and ultrasonic activation. The mechanism of cyanide removal by persulfate was also discussed.

2. Materials and Methods

2.1. Materials and Chemicals

In this study, the gold cyanide residue produced by a gold enterprise in Shandong province (China) was used. The XRD analysis of the gold cyanide residue shown in Figure 1 reveals that the main minerals were quartz and pyrite, indicating that Si, S and Fe were the main elements combining with chemical analysis (Table 1). Table 2 shows the cyanide contents in the cyanide residue and toxic leaching solution. The content of total cyanide was much higher than free cyanide, showing that there were plenty of stable metal complex cyanides. The moisture content of the cyanide residue was about 15%. Over 90% of mineral particles in the cyanide residue were smaller than 40 μm.

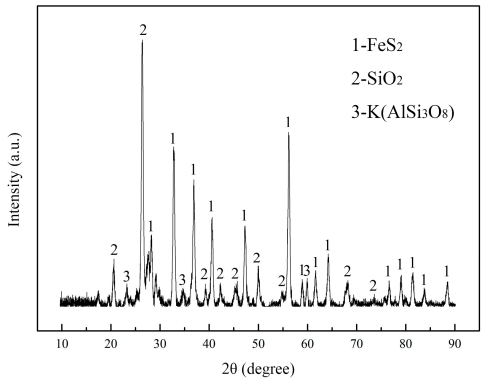


Figure 1. XRD analysis of gold cyanide residue.

Table 1. Chemical analysis of gold cyanide residue (wt.%).

Parameter	Si	S	Fe	Zn	Pb	Cu	Others
Value	34.5	27.1	22.3	0.69	0.62	0.43	14.36

Table 2. The cyanide content analysis of gold cyanide residue.

Parameter	Cyanide Residue (mg/kg)		Toxic Leaching Solution (mg/L)	
	Total Cyanide	Free Cyanide	Total Cyanide	Free Cyanide
Value	1600 ± 100	220 ± 10	65 ± 5	23 ± 2

Analytical-grade sodium hydroxide NaOH (Damao, Tianjin, China) was used to adjust pH. Analyticalgrade potassium persulfate $K_2S_2O_8$ (Damao, Tianjin, China) was used as the oxidizing agent. Analytical-grade tert-butanol and methanol (Damao, Tianjin, China) were used as the scavengers of free radicals.

2.2. Removal of Cyanide in Cyanide Residue

The schematic diagram of the experimental process of cyanide removal is shown in Figure 2. All the experiments were carried out in duplicate, and values presented are the average of both results. Cyanide residue slurry (30 wt.%) was prepared with deionized water in a 300 mL beaker with mechanical agitation. The pH of the slurry was adjusted with NaOH (range from 8.0 to 12.0) and measured with a pH meter (pHS-3E, BIOBASE, Shanghai, China). Then, the slurry was heated to the operating temperature, which was in the range of 20 °C to 80 °C. The cyanide removal experiments were carried out using magnetic stirrer with agitation at 150 rpm (SXJB-500, Ronghui, Shanghai, China) or ultrasonic apparatus (KQ-250DE, Kunshan, China, ultrasonic power 250 W, ultrasonic frequency 40 KHZ). The experiment started when a certain amount of $K_2S_2O_8$ (0~5 wt.%) was added simultaneously to the slurry. The slurry was separated through centrifugation after cyanide removal, and then the contents of total cyanide in the residue and filtrate were determined through the silver nitrate titration method [27,28]. Cyanide removal efficiency (η) was calculated according to the following equation:

$$\eta = \frac{w_1 - w_2}{w_1} \times 100\% \quad (1)$$

where w_1 (mg/kg) and w_2 (mg/kg) represent the contents of total cyanide in the cyanide residue before and after the cyanide removal process, respectively. In addition, the content of total cyanide in the toxic leaching solution of the specific cyanide residue was also determined [29].

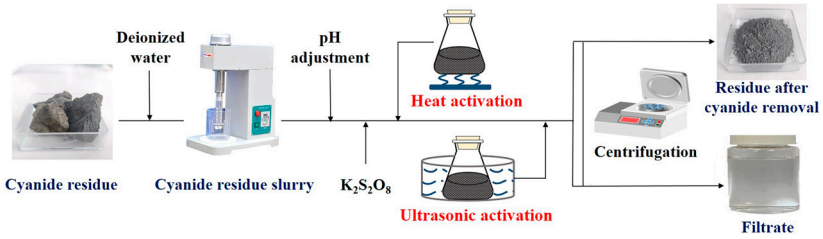


Figure 2. Schematic diagram of experimental process of cyanide removal.

3. Results and Discussion

3.1. Effect of pH

In this section, the effect of pH on the removal of cyanide by persulfate is evaluated. Considering the initial pH of the slurry (7.5–8.0), the pH was varied from 8.0 to 12.0 under the following conditions: $K_2S_2O_8$ = 2.0 wt.%, T = 20 °C and time = 60 min. Figure 3 shows the cyanide removal efficiency from the cyanide residue and the total cyanide content in the filtrate of the slurry. The results show a significant efficiency increase at pH 10.0 (50.61%), which then decreased as the pH increased from this point onwards. Under slightly alkaline conditions, free radical $SO_4^{\bullet -}$ was produced through the decomposition of

persulfate. With the higher alkalinity, $SO_4^{\bullet -}$ and OH^- transformed into SO_4^{2-} and $HO^{\bullet}$, as shown in Equation (2) [30].

$$SO_4^{\bullet -} + OH^- \rightarrow HO^{\bullet} + SO_4^{2-} \quad (2)$$

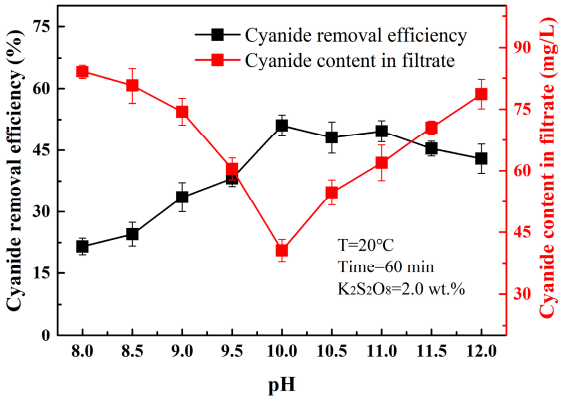


Figure 3. Effect of pH on cyanide removal through $S_2O_8^{2-}$ oxidation.

It was reported that $SO_4^{\bullet -}$ was the more dominant radical when pH < 7, while $SO_4^{\bullet -}$ and $HO^{\bullet}$ both predominated at pH = 9. When pH > 12, $HO^{\bullet}$ radical reacted dominantly [15]. For the treatment of some pollutants, the low pH was used to achieve a high degradation rate by the stronger oxidant $SO_4^{\bullet -}$ [31]. However, the initial pH could not be too low, in order to avoid the leakage of toxic HCN gas from the treatment of cyanide. It is worth noting that the cyanide content in the filtrate increased with the pH increasing from 10.0 to 12.0. In the process, free cyanides were produced from the decomposition of metal complex cyanides and moved from the residue to the filtrate. Under the condition of high pH, the cyanide in the filtrate could not be removed effectively because the oxidation of cyanide by $HO^{\bullet}$ was weaker than $SO_4^{\bullet -}$. According to the results in Figure 3, the initial pH of the slurry should be set at 10.0 to achieve maximum efficiency.

3.2. Effect of Persulfate Addition

In this section, the $K_2S_2O_8$ dose was varied in the range 0.5~5.0 wt.% under the following conditions: pH = 10.0, T = 20 °C and time = 60 min. The results are shown in Figure 4. The cyanide removal efficiency increased with increasing $K_2S_2O_8$ addition from 0.5 wt.% to 2.0 wt.%. The $K_2S_2O_8$ dose of 2.0 wt.% was over three times that of the theoretical amount calculated using Equation (3), suggesting that part of the excess persulfate reacted with pyrite in the cyanide residue. Persulfate was also considered as a kind of radical scavenger (Equations (4) and (5)); the higher dose of persulfate resulted in weak oxidability, and as shown in Figure 4, the efficiency decreased with the $K_2S_2O_8$ dose over 2.0 wt.%. On the other hand, the content of cyanide in the filtrate increased when the $K_2S_2O_8$ addition was over 0.5 wt.%. $S_2O_8^{2-}$ with high concentration began to oxidize pyrite, with the result that the free cyanides generated through the decomposition of complex cyanides could not be removed effectively. These cyanides could be absorbed into the residue by the surface of the cyanide residue or remain in the filtrate, leading to the increase in cyanide content in both residue and filtrate. In practical production, filtrate with a high content of cyanide could be recovered and returned to the cyanidation process for secondary utilization. Taken together, the $K_2S_2O_8$ dose of 2.0 wt.% was best for the cyanide removal of gold cyanide residues.

$$S_2O_8^{2-} + CN^- + 2OH^- \rightarrow 2SO_4^{2-} + CNO^- + H_2O \quad (3)$$

$$S_2O_8^{2-} + SO_4^{\bullet -} \rightarrow S_2O_8^{\bullet -} + SO_4^{2-} \quad (4)$$

$$S_2O_8^{2-} + HO^{\bullet} \rightarrow S_2O_8^{\bullet -} + OH^- \quad (5)$$

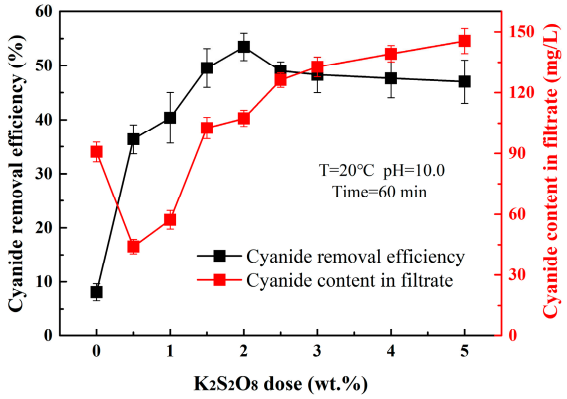


Figure 4. Effect of persulfate addition on cyanide removal through $S_2O_8^{2-}$ oxidation.

3.3. Effect of Reaction Time

As one of the advanced oxidation processes, persulfate oxidation has the advantage of a rapid reaction. To investigate the reaction rate of cyanide removal through persulfate oxidation, the experiments were carried out with a reaction time of 15~180 min, under the conditions of pH = 10.0, T = 20 °C, $K_2S_2O_8$ = 2.0 wt.%. The results are shown in Figure 5. It was demonstrated that cyanide removal efficiency increased significantly during the first 15 min and reached its highest at 60 min. It was speculated that the reaction essentially ended after 60 min, as not only were no new free radicals generated, but also the amount of free radical quenching increased, resulting in a decrease in cyanide removal efficiency. The cyanide content in the filtrate increased gradually until 90 min. It was also found that there was, respectively, 1.43 g/L, 2.54 g/L, 2.03 g/L and 1.94 g/L Fe^{3+} in the filtrate at the reaction time of 30, 60, 90 and 120 min. When the content of Fe^{3+} and cyanide in slurry reached a certain level, $Fe_4[Fe(CN)_6]_3$ precipitation formed and entered into the residue, decreasing the content of Fe^{3+} in the liquid phase and the cyanide removal efficiency of the residue after 60 min. According to the results in Figure 5, the time of the cyanide removal process should be set at 60 min.

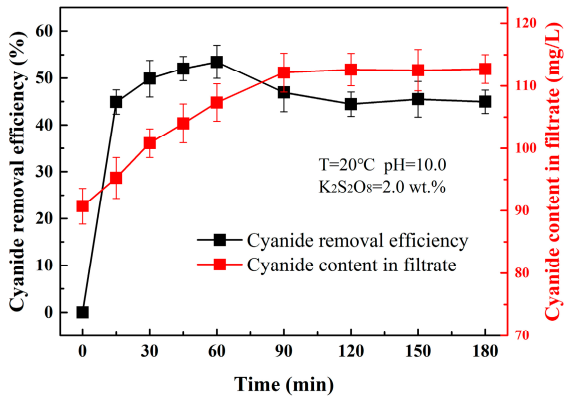


Figure 5. Effect of reaction time on cyanide removal through $S_2O_8^{2-}$ oxidation.

3.4. Heat Activation

In this section, cyanide removal was studied under different temperatures (20 °C to 80 °C) and under conditions of pH = 10.0, $K_2S_2O_8$ = 2.0 wt.% and time = 60 min. It is shown in Figure 6 that 60 °C was the most efficient temperature, with 62.18% removal efficiency, indicating that the cyanide removal was promoted by heat activation. Two pathways were put forward to explain the generation of sulfate radicals ($SO_4^{\bullet -}$) by heat-activated persulfate,

as shown in Equations (6) and (7). The first is that one persulfate ion produces two sulfate radicals using heat energy, and the second is that an electron donor reacts with an ion, generating a single sulfate radical, like the pathway of metal-activated persulfate [32]. At present, lots of studies have shown that heat activation was more effective than metal activation, so the first pathway (Equation (6)) has been generally considered to be the pathway of heat activation [33,34]. In this way, 1 mol persulfate could generate 2 mol $SO_4^{\bullet -}$ through fracturing O-O bond with a thermal activation energy of 140.02 kJ/mol [15]. The cyanide removal efficiency could be increased by a small increase in temperature.

$$S_2O_8^{2-} + \text{heat} \rightarrow 2SO_4^{\bullet -} \quad (6)$$

$$S_2O_8^{2-} + e^- \rightarrow SO_4^{\bullet -} + SO_4^{2-} \quad (7)$$

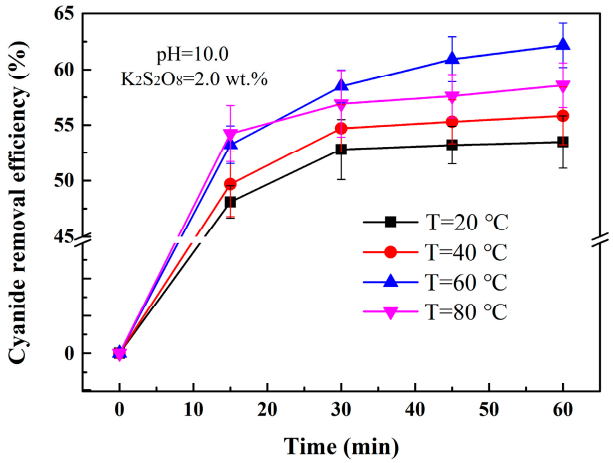


Figure 6. Cyanide removal efficiency of cyanide residue through heat-activated persulfate process.

It is shown in Figure 6 that cyanide removal efficiency decreased with the temperature increasing from 60 °C to 80 °C. When the temperature was too high, plenty of $SO_4^{\bullet -}$ was generated at the same time. Then, some of the free radicals would be quenched when spreading in slurry, which could not react with cyanide in a short time [35]. The degradation of cyanide by heat-activated persulfate reached saturation at a certain temperature, like most pollutants [36].

3.5. Ultrasonic Activation

Ultrasonic activation refers to the production of active substances through the expansion and collapse of the cavities under the influence of sound field. The phenomenon is also called acoustic cavitation [37]. Ultrasound could improve the degradation of pollutants by promoting the generation of free radicals and mass transfer among reactants [38]. To investigate the effect of ultrasonic activation on the treatment of cyanide residue, cyanide removal experiments were carried out under the conditions of different ultrasonic power (0, 40%, 70% and 100%), T = 20 °C, initial pH = 10.0, $K_2S_2O_8$ dose = 2.0 wt.% and time = 60 min. The results in Figure 7 show that the maximum cyanide removal efficiency reached 74.76% under the condition of ultrasonic power = 100%, which is 12.58% more than that of heat activation in Section 3.4. This indicates that the generation of free radicals for cyanide removal was promoted by the increasing number of collapsing bubbles during the ultrasonic activation process. The lowest cyanide content in the toxic leaching solution of the residue after the ultrasonic-activated persulfate-advanced oxidation process was 3.84 mg/L < 5 mg/L, meeting the national standard (HJ943-2018, China).

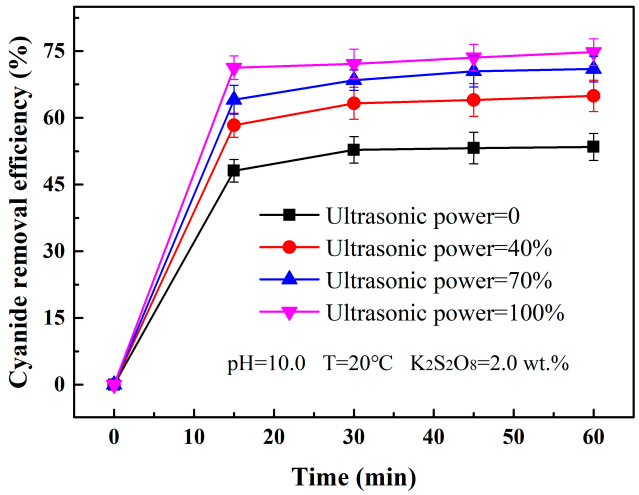


Figure 7. Cyanide removal efficiency through ultrasonic-activated persulfate process.

3.6. Mechanism Analysis of Cyanide Removal through Activated $S_2O_8^{2-}$ Process

3.6.1. Generation of Free Radicals

Tert-butanol and methanol are two common free radical scavengers. Studies have shown that the reaction rates of $SO_4^{\bullet-}$ and $HO^{\bullet}$ with tert-butanol are 4.0×10^5 $M^{-1} \cdot s^{-1}$ and 1.1×10^7 $M^{-1} \cdot s^{-1}$, respectively, while the reaction rates of $SO_4^{\bullet-}$ and $HO^{\bullet}$ with methanol are 3.2×10^6 $M^{-1} \cdot s^{-1}$ and 9.7×10^8 $M^{-1} \cdot s^{-1}$, respectively [26]. Therefore, tert-butanol is mainly a scavenger of $HO^{\bullet}$ radicals, while methanol can be a scavenger of both $SO_4^{\bullet-}$ and $HO^{\bullet}$ radicals. In this section, the cyanide removal efficiencies of different treatment processes (Table 3) with and without free radical scavengers are shown in Figure 8. The amount of tert-butanol and methanol added was 2.0 wt.%. The cyanide removal efficiency decreased with the addition of both tert-butanol and methanol when $S_2O_8^{2-}$ existed in the systems, showing that both $SO_4^{\bullet-}$ and $HO^{\bullet}$ were generated during the $S_2O_8^{2-}$ process. The results show little difference between the treatments with the two kinds of radical scavengers added, indicating that $HO^{\bullet}$ played a major role in cyanide removal. It could be inferred that more free radicals were generated through ultrasonic activation due to the higher reduction in the cyanide removal efficiency with radical scavengers. It is worth noting that when $S_2O_8^{2-}$ did not exist in the systems, only 16.54% of cyanides in the residue were removed through ultrasonic treatment. There might be two reasons for this: that (1) some of the cyanides in the residue were removed into the filtrate through ultrasonic shaking and (2) $HO^{\bullet}$ radical was generated in aqueous solution by ultrasound and then oxidized cyanide [39]. The study of Wei et al. [40] found that the amount of $HO^{\bullet}$ generated was about twice as much as $SO_4^{\bullet-}$ in the ultrasonic-activated persulfate process because cavitation bubbles enhanced the reactions between sulfate radicals and water molecules.

Table 3. Conditions of different treatment processes.

Treatment Process	pH	Persulfate Addition (wt.%)	Reaction Time (min)	Temperature (°C)	Ultrasonic Power (%)
$S_2O_8^{2-}$	10.0	2.0	60	20	0
US	10.0	0	60	20	100
$S_2O_8^{2-}$/Heat	10.0	2.0	60	60	0
$S_2O_8^{2-}$/US	10.0	2.0	60	20	100

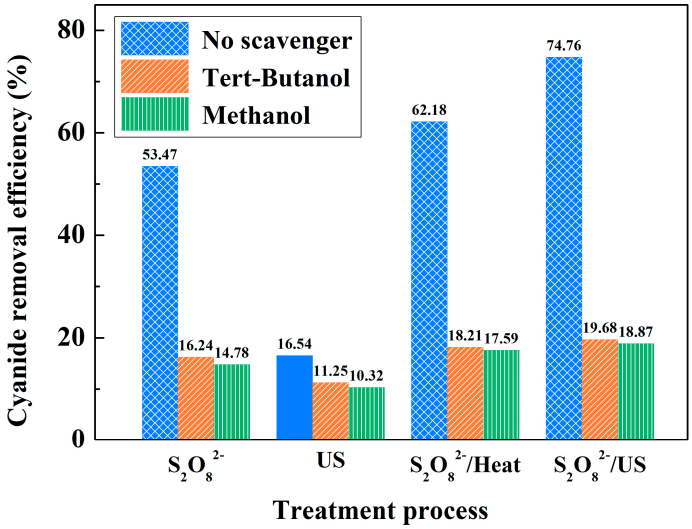


Figure 8. Comparison of cyanide removal efficiency through different treatment processes.

3.6.2. XPS Analysis

To determine the change in the main species during the cyanide removal process, the XPS spectra (survey, Fe 2p, S 2p and N 1s) of cyanide residue before and after cyanide removal treatment are shown in Figures 9 and 10 and Table 4. Sample A is the original cyanide residue before cyanide removal treatment, and Samples B and C are residues after treatment through the heat-activated and ultrasonic-activated persulfate process, respectively. The results show that the content of C on the surface of the cyanide residue before treatment was 23.13% and, respectively, decreased to 19.36% and 16.68% in Sample B and Sample C. The N element was only detected on the surface of the original cyanide residue. The change in elements C and N content showed that the cyanide adsorbed on the surface of the cyanide residue was effectively removed through the persulfate-advanced oxidation process.

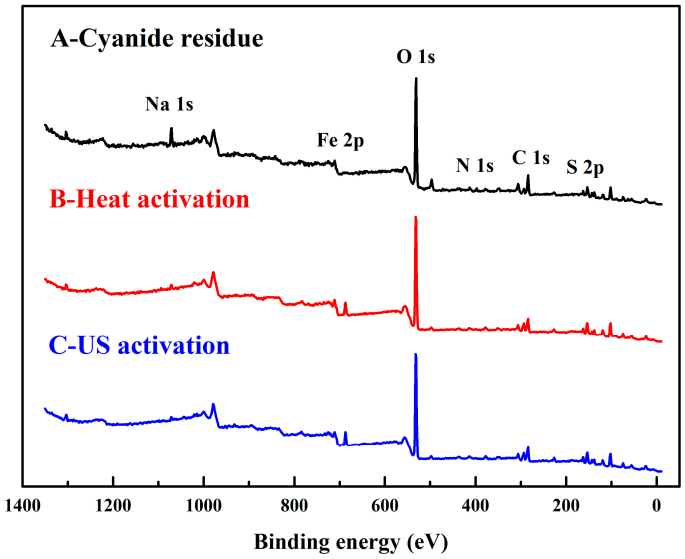


Figure 9. XPS survey spectra of cyanide residues before and after cyanide removal treatment.

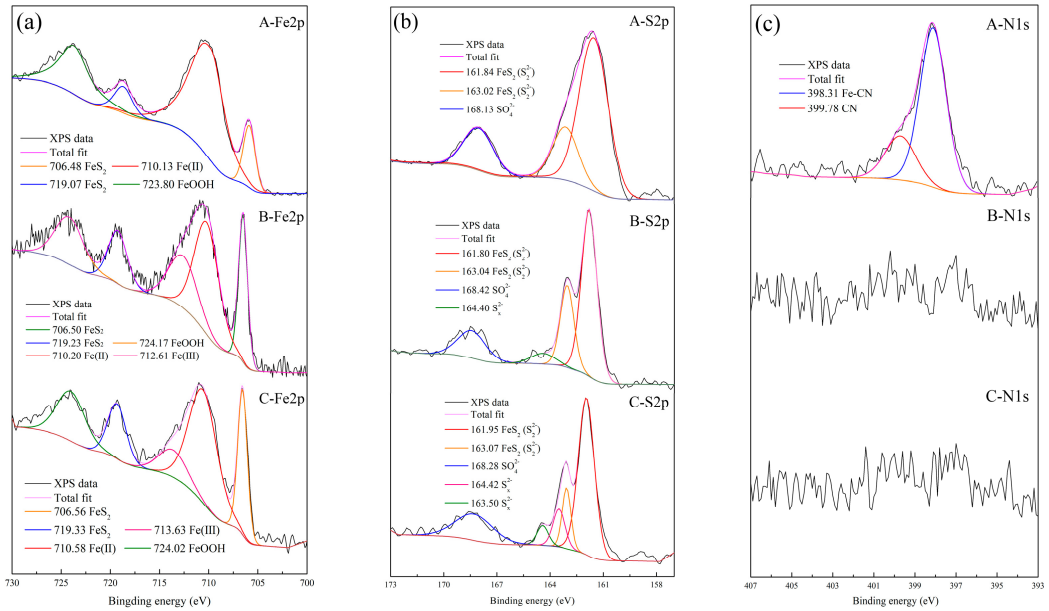


Figure 10. XPS spectra of the cyanide residue before and after cyanide removal treatment: (**a**) Fe2p, (**b**) S2p, (**c**) N1s.

Table 4. Atomic concentrations of main elements on surface of cyanide residues.

Samples	Name	Peak BE (eV)	Atomic (%)
A	Fe 2p	711.10	3.78
	O 1s	531.20	44.81
	C 1s	284.09	23.13
	S 2p	162.33	2.87
	N 1s	397.46	2.77
B	Fe 2p	711.11	2.70
	O 1s	531.61	54.72
	C 1s	284.31	19.36
C	Fe 2p	710.64	3.23
	O 1s	531.60	50.89
	C 1s	284.24	16.71

Figure 10 shows that there was mainly pyrite (FeS_2), Fe(II), FeOOH and $SO_4{}^2-$ on the surface of cyanide residues obtained after cyanidation [41,42]. The cyanides adsorbed on the surface were mainly iron–cyanide complex cyanide (Fe−CN), with a small amount of free cyanide (CN^-) [43]. It is shown in Figure 10a that the proportion of pyrite and Fe(II) decreased, and Fe(III) appeared after the heat-activated and ultrasonic-activated persulfate treatment, respectively accounting for 12.54% and 9.92% [44]. The XPS spectra of S2p (Figure 10b) show that there were various forms of polysulfide ($S_x{}^{2-}$) appearing on the surface of the residues after cyanide removal, which was caused by the incomplete oxidation of pyrite. Compared with heat activation, the proportion of Fe(III) produced through the ultrasonic activation treatment was lower and the proportion of $S_x{}^{2-}$ was higher, indicating that the oxidation degree of pyrite during the ultrasonic-activated $S_2O_8{}^{2-}$ process was lower than that of the heat-activated process. In Figure 10c, the N1s peak of residues after cyanide removal is cluttered with low intensity, leading to invalid detection results. It also shows that the cyanide in the gold cyanide residue was clearly removed through persulfate treatment.

3.6.3. Oxidation of Pyrite

The cyanide removal efficiency was seriously affected by the side reactions of other substances in the cyanide residues, of which the main reaction was the oxidation of pyrite. According to the XPS results, the pyrite was mainly oxidized to Fe^{3+} during the cyanide removal process. Figure 11 shows the content of Fe^{3+} in slurry after different treatment processes. The Fe^{3+} content decreased in two kinds of activation processes with the addition of tert-butanol and methanol, showing that the free radicals generated by activated persulfate also participated in the oxidation of pyrite. However, the amount of free radicals reacting with pyrite during the ultrasonic activation process was less than that of heat activation, and the reactions were more concentrated in the oxidation with cyanide. In the actual production process, flotation recovery of valuable elements in cyanide residue was carried out after cyanide removal, so there should not be too much loss of Fe during the cyanide process. The loss caused by the reaction between pyrite and cyanide removal agents should be reduced while ensuring the efficient removal of cyanide. Clearly, ultrasonic activation technology can better meet this requirement.

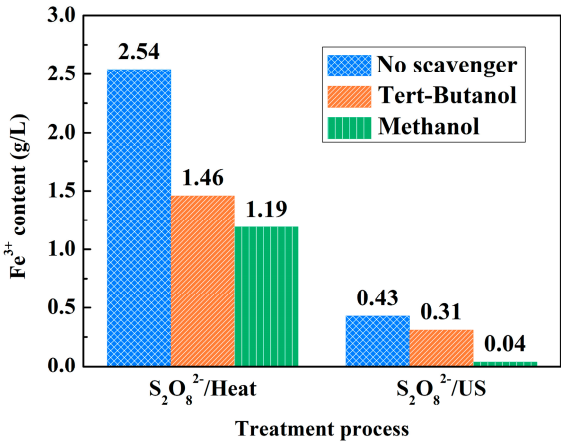


Figure 11. Comparison of Fe^{3+} content for different treatment processes.

3.6.4. Transfer of Cyanide

There are two main pathways to remove cyanide in cyanide gold residues: the first is by chemical reactions that change cyanide into harmless substances and the second is to transfer cyanide from the residue to the liquid phase in slurry through dissolution or other methods. The total cyanide contents in the filtrate after different treatment processes (Figure 12) showed that there was 107.33 mg/L cyanide in the filtrate after the $S_2O_8^{2-}$/heat process, higher than the $S_2O_8^{2-}$ process. The main reason is that more complex cyanides were decomposed through oxidation and then entered to the liquid phase. The contents of cyanide in the filtrate after the stirring treatment, US without persulfate process and $S_2O_8^{2-}$/US process were, respectively, 90.74 mg/L, 137.2 mg/L and 211.68 mg/L, indicating that ultrasound promoted the transfer of cyanide from the residue to the liquid phase. The energy generated by ultrasound destroyed the bond in complex cyanide, making the transfer easier. In industrial production, the wastewater containing cyanide can be returned to the cyanidation system for secondary use, so it is also an efficient way to treat gold cyanide residues by transferring cyanide from the residue into the liquid phase as much as possible.

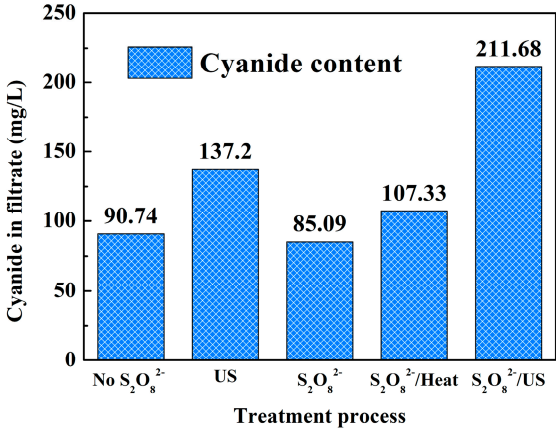


Figure 12. Comparison of cyanide content in filtrate for different treatment processes.

4. Conclusions

The removal of cyanide in cyanide residues by persulfate was carried out in this study. The results showed that with the application of the operational conditions pH = 10.0, $K_2S_2O_8$ = 2.0 wt.%, temperature = 60 °C, agitation = 150 rpm and time = 60 min, cyanide removal efficiency reached 62.18%. It was also shown that the application of ultrasound at 20 °C reached 74.76% removal. It is concluded that these two processes are very efficient. The mechanism study investigated the reasons behind the high efficiency of the ultrasonic-activated persulfate-advanced oxidation process. (1) Free radicals ($SO_4^{\bullet -}$ and $HO^{\bullet}$) that could accelerate the oxidation of cyanide were generated in the persulfate activation process, and $HO^{\bullet}$ played a major role under alkaline conditions. (2) As the main side reaction during the treatment of cyanide residue, the oxidation of pyrite was reduced. The ultrasonic-activated persulfate focused on the removal of cyanide. (3) In addition to oxidation by persulfate and free radicals, more cyanides were removed by transferring from the cyanide residue to the liquid phase by the ultrasonic shock. The cyanide content in the toxic leaching solution of the residue was under the national standard (HJ943-2018, China) after cyanide removal through the ultrasonic-activated persulfate-advanced oxidation process, which has potential application prospects for the treatment of gold cyanide residues.

Author Contributions: Conceptualization, W.H.; methodology, W.H.; formal analysis, W.H.; investigation, W.H.; resources, H.Y. and L.T.; writing—original draft, W.H.; visualization, H.Y. and L.T.; funding acquisition, H.Y. All authors have read and agreed to the published version of the manuscript.

Funding: This study was financially supported by the National Natural Science Foundation of China (52274348), Major projects for the "Revealed Top" Science and Technology of Liaoning Province (2022JH1/10400024) and National Key R&D Program of China (2018YFC1902002).

Data Availability Statement: Data that support the findings of this study are available from the corresponding author upon reasonable request.

Conflicts of Interest: The authors declare no conflict of interest.

References

1. Deschênes, G. Advances in the cyanidation of gold. *Dev. Miner. Process.* **2005**, *20*, 479–500.
2. Medina, D.; Anderson, C.G. A review of the cyanidation treatment of copper-gold ores and concentrates. *Metals* **2020**, *10*, 897. [CrossRef]
3. Ma, Y.W.; Han, Y.X.; Zhu, Y.M.; Li, Y.J.; Liu, H. Flotation behaviors and mechanisms of chalcopyrite and galena after cyanide treatment. *TNMSC* **2016**, *26*, 3245–3252. [CrossRef]
4. Hewwitt, D.; Breuer, P.; Jeffery, C. Cyanide detoxification of gold cyanidation tails and process streams. *Miner. Process. Extr.* **2012**, *121*, 228–236. [CrossRef]
5. *HJ943-2018*; Technical Specification for Pollution Control of Cyanide Leaching Residue in Gold Industry. Ministry of Environmental Protection of the People's Republic of China: Beijing, China, 2018.

6. Akcil, A. Destruction of cyanide in gold mill effluents: Biological versus chemical treatments. *Biotechnol. Adv.* **2003**, *21*, 501–511. [CrossRef]
7. Anning, C.; Wang, J.; Chen, P.; Batmunkhi, I.; Lyu, X. Determination and detoxification of cyanide in gold mine tailings: A review. *Waste Manag. Res.* **2019**, *37*, 1117–1126. [CrossRef]
8. Kuyucak, N.; Akcil, A. Cyanide and removal options from effluents in gold mining and metallurgical processes. *Miner. Eng.* **2013**, *50–51*, 13–29. [CrossRef]
9. Guo, X.; Jiang, X.; Zhu, J.; Liu, Q.; Zhang, Y.; Liu, X. Deep treatment technology for cyanidation barren solution from a gold enterprise. *Gold* **2019**, *40*, 64–67.
10. Xiong, Q.; Jiang, S.; Fang, R.; Liu, S.; Wu, X. An environmental-friendly approach to remove cyanide in gold smelting pulp by chlorination aided and corncob biochar: Performance and mechanisms. *J. Hazard. Mater.* **2021**, *408*, 124465. [CrossRef]
11. Kitis, M.; Akcil, A.; Karakaya, E.; Yigit, N.O. Destruction of cyanide by hydrogen peroxide in tailings slurries from low bearing sulphidic gold ores. *Miner. Eng.* **2005**, *18*, 353–362. [CrossRef]
12. Sánchez-Castillo, M.A.; Carrillo-Pedroza, F.R.; Fraga-Tovar, F.; Soria-Aguilar, M.D.J. Ozonation of Cyanide Catalyzed by Activated Carbon. Ozone. *Sci. Eng.* **2015**, *37*, 240–251.
13. Tu, Y.; Han, P.; Wei, L.; Zhang, X.; Yu, B.; Qian, P.; Ye, S. Removal of cyanide adsorbed on pyrite by H_2O_2 oxidation under alkaline conditions. *J. Environ. Sci.* **2019**, *78*, 287–292. [CrossRef] [PubMed]
14. Ma, D.; Yi, H.; Lai, C.; Liu, X.; Huo, X.; An, Z.; Li, L.; Fu, Y.; Li, B.; Zhang, M.; et al. Critical review of advanced oxidation processes in organic wastewater treatment. *Chemosphere* **2021**, *275*, 130104. [CrossRef] [PubMed]
15. Koppenol, W.H. Names for inorganic radicals (IUPAC Recommendations 2000). *Pure Appl. Chem.* **2000**, *72*, 437–446. [CrossRef]
16. Ike, I.A.; Linden, K.G.; Orbell, J.D.; Duke, M. Critical review of the science and sustainability of persulphate advanced oxidation processes. *Chem. Eng. J.* **2018**, *338*, 651–669. [CrossRef]
17. Huang, W.; Xiao, S.; Zhong, H.; Yan, M.; Yang, X. Activation of persulfates by carbonaceous materials: A review. *Chem. Eng. J.* **2021**, *418*, 129297. [CrossRef]
18. Qi, C.; Liu, X.; Lin, C.; Zhang, X.; Ma, J.; Tan, H.; Ye, W. Degradation of sulfamethoxazole by microwave-activated persulfate: Kinetics, mechanism and acute toxicity. *Chem. Eng. J.* **2014**, *249*, 6–14.
19. Hori, H.; Nagano, Y.; Murayama, M.; Koike, K.; Kutsuna, S. Efficient decomposition of perfluoroether carboxylic acids in water with a combination of persulfate oxidant and ultrasonic irradiation. *J. Fluor. Chem.* **2012**, *141*, 5–10. [CrossRef]
20. Darsinou, B.; Frontistis, Z.; Antonopoulou, M.; Konstantinou, I.; Mantzavinos, D. Sono-activated persulfate oxidation of bisphenol A: Kinetics, pathways and the controversial role of temperature. *Chem. Eng. J.* **2015**, *280*, 623–633. [CrossRef]
21. Arvaniti, O.S.; Bairamis, F.; Konstantinou, I.; Mantzavinos, D.; Frontistis, Z. Degradation of antihypertensive drug valsartan in water matrices by heat and heat/ultrasound activated persulfate: Kinetics, synergy effect and transformation products. *Chem. Eng. J. Adv.* **2020**, *4*, 100062. [CrossRef]
22. Monteagudo, J.M.; El-taliawy, H.; Durán, A.; Caro, G.; Bester, K. Sono-activated persulfate oxidation of diclofenac: Degradation, kinetics, pathway and contribution of the different radicals involved. *J. Hazard. Mater.* **2018**, *357*, 457–465. [CrossRef] [PubMed]
23. Wang, S.; Zhou, N. Removal of carbamazepine from aqueous solution using sono-activated persulfate process. *Ultrason. Sonochem.* **2016**, *29*, 156–162. [CrossRef] [PubMed]
24. Hossein Panahi, A.; Meshkinian, A.; Ashrafi, S.D.; Khan, M.; Naghizadeh, A.; Abi, G.; Kamani, H. Survey of sono-activated persulfate process for treatment of real dairy wastewater. *Int. J. Environ. Sci. Technol.* **2020**, *17*, 93–98. [CrossRef]
25. Sun, X.B.; Zhao, Y.Y.; Liu, Y.D.; Fu, D. A new approach to the treatment of ferricyanide wastewater with persulfate. *J. Saf. Environ.* **2018**, *18*, 1463–1467.
26. Moussavi, G.; Pourakbar, M.; Aghayani, E.; Mahdavianpour, M. Investigating the aerated VUV/PS process simultaneously generating hydroxyl and sulfate radicals for the oxidation of cyanide in aqueous solution and industrial wastewater. *Chem. Eng. J.* **2018**, *350*, 673–680. [CrossRef]
27. *TCG/A 013-2019*; Method for Chemical Analysis of Cyanide Leaching Residue in Gold Industry-Determination of Cyanide-Titration and Spectrophotometry Method. China Gold Association: Beijing, China, 2019.
28. *HJ484-2009*; Water Quality-Determination of Cyanide-Volumetric and Spectrophotometry Method. Ministry of Environmental Protection of the People's Republic of China: Beijing, China, 2009.
29. *HJ/T299-2007*; Solid Waste-Extraction Procedure for Leaching Toxicity Sulphuric Acid & Nitric Acid Method. Ministry of Environmental Protection of the People's Republic of China: Beijing, China, 2007.
30. Furman, O.S.; Teel, A.L.; Watts, R.J. Mechanism of base activation of persulfate. *Environ. Sci. Technol.* **2010**, *44*, 6423–6428. [CrossRef] [PubMed]
31. Goulden, P.D.; Anthony, D.H.J. Kinetics of uncatalyzed peroxydisulfate oxidation of organic material in fresh water. *Anal. Chem.* **1978**, *50*, 953–958. [CrossRef]
32. Matzek, L.W.; Carter, K.E. Activated persulfate for organic chemical degradation: A review. *Chemosphere* **2016**, *151*, 178–188. [CrossRef]
33. Zhao, D.; Liao, X.; Yan, X.; Huling, S.G.; Chai, T.; Tao, H. Effect and mechanism of persulfate activated by different methods for PAHs removal in soil. *J. Hazard. Mater.* **2013**, *254–255*, 228–235.
34. Deng, D.; Peng, L.; Guan, M.; Kang, Y. Impact of activation methods on persulfate oxidation of methyl tert-butyl ether. *J. Hazard. Mater.* **2014**, *264*, 521–528. [CrossRef]

35. Lin, Y.Q. Application of Persulfate Activated Advanced Oxidation Technology in Wastewater Treatment. Ph.D. Thesis, Changchun University of Science and Technology, Changchun, China, 2020.
36. Hori, H.; Nagaoka, Y.; Murayama, M.; Kutsuna, S. Efficient decomposition of perfluorocarboxylic acids and alternative fluorochemical surfactants in hot water. *Environ. Sci. Technol.* **2008**, *42*, 7438–7443. [CrossRef] [PubMed]
37. Frontistis, Z.; Mantzavinos, D. Sonodegradation of 17α-ethynylestradiol in environmentally relevant matrices: Laboratory-scale kinetic studies. *Ultrason. Sonochem.* **2012**, *19*, 77–84. [CrossRef] [PubMed]
38. Frontistis, Z. Degradation of the nonsteroidal Anti-Inflammatory drug piroxicam by Iron activated persulfate: The role of water matrix and ultrasound synergy. *Int. J. Environ. Res. Public Health* **2018**, *15*, 2600. [CrossRef]
39. Yazıcı, E.Y.; Deveci, H.; Alp, I.; Uslu, T. Generation of hydrogen peroxide and removal of cyanide from solutions using ultrasonic waves. *Desalination.* **2007**, *216*, 209–221. [CrossRef]
40. Wei, Z.; Villamena, F.A.; Weavers, L.K. Kinetics and mechanism of ultrasonic activation of persulfate: An in Situ EPR spin trapping study. *Environ. Sci. Technol.* **2017**, *51*, 3410–3417. [CrossRef] [PubMed]
41. Zhang, X.; Han, Y.; Gao, P.; Li, Y.; Sun, Y. Effects of particle size and ferric hydroxo complex produced by different grinding media on the flotation kinetics of pyrite. *Powder Technol.* **2020**, *360*, 1028–1036. [CrossRef]
42. Mu, Y.; Li, L.; Peng, Y. Surface properties of fractured and polished pyrite in relation to flotation. *Miner. Eng.* **2017**, *101*, 10–19. [CrossRef]
43. Nie, Q.; Wang, M.; Qiu, T.; Qiu, X. Density functional theory and XPS studies of the adsorption of cyanide on chalcopyrite surfaces. *ACS Omega* **2020**, *5*, 22778–22785. [CrossRef]
44. Cheng, M.; Liu, Y.; Huang, D.; Lai, C.; Zeng, G.; Huang, J.; Liu, Z.; Zhang, C.; Zhou, C.; Qin, L.; et al. Prussian blue analogue derived magnetic Cu-Fe oxide as a recyclable photo-Fenton catalyst for the efficient removal of sulfamethazine at near neutral pH values. *Chem. Eng. J.* **2019**, *362*, 865–876. [CrossRef]

Disclaimer/Publisher's Note: The statements, opinions and data contained in all publications are solely those of the individual author(s) and contributor(s) and not of MDPI and/or the editor(s). MDPI and/or the editor(s) disclaim responsibility for any injury to people or property resulting from any ideas, methods, instructions or products referred to in the content.